RESEARCH ARTICLE | MARCH 01 2022

Analytical prediction of electrowetting-induced jumping motion for droplets on textured hydrophobic substrates: Effects of the wetting states

Kaixuan Zhang (张凯旋) ; Jiayi Zhao (赵嘉毅) ; Yang Liu (刘扬); Shuo Chen (陈硕)

Physics of Fluids 34, 032001 (2022)
https://doi.org/10.1063/5.0082832

Physics of Fluids ARTICLE scitation.org/journal/phf

Analytical prediction of electrowetting-induced jumping motion for droplets on textured hydrophobic substrates: Effects of the wetting states

Cite as: Phys. Fluids **34**, 032001 (2022); doi: 10.1063/5.0082832
Submitted: 19 December 2021 · Accepted: 10 February 2022 ·
Published Online: 1 March 2022

View Online Export Citation CrossMark

Kaixuan Zhang (张凯旋),[1,2] Jiayi Zhao (赵嘉毅),[3] Yang Liu (刘扬),[4] and Shuo Chen (陈硕)[1,a)]

AFFILIATIONS

[1]School of Aerospace Engineering and Applied Mechanics, Tongji University, Shanghai 200092, China
[2]Institute of Biomechanics and Medical Engineering, AML, Department of Engineering Mechanics, Tsinghua University, Beijing 100084, China
[3]School of Energy and Power Engineering, University of Shanghai for Science and Technology, Shanghai 200093, China
[4]Department of Mechanical Engineering, The Hong Kong Polytechnic University, Hung Hom, Kowloon, Hong Kong

[a)]**Author to whom correspondence should be addressed:** schen_tju@mail.tongji.edu.cn

ABSTRACT

In electrowetting, an applied electric voltage can induce spreading, sliding, or even jumping of an individual droplet by changing the intrinsic balance of the three-phase interfacial tensions. This technique has been widely used for manipulating droplets in microfluidics and by lab-on-a-chip devices in recent decades. In the present paper, we present an analytical prediction of the jumping velocity for droplets undergoing electrowetting on textured hydrophobic surfaces with different wetting states. In particular, we consider wetting a liquid droplet on a textured hydrophobic substrate with a voltage applied between the droplet and the substrate. Once the voltage is turned off, the energy stored in the droplet during electrowetting is released and could even result in the detachment of the droplet. The effects of the initial and electrowetting states, i.e., the Cassie–Baxter state and the Wenzel state, on the jumping velocity of droplets are systematically discussed. Based on energy conservation, the energy conversion between the surface energy, the elastic energy of the contact line, and the kinetic energy of droplets due to internal viscous dissipation in different wetting states is analyzed. Closed-form formulas for the jumping velocity of different droplet wetting states are systematically derived. Finally, a unified form for predicting the electrowetting-induced jumping velocity of droplets on both flat and textured substrates with different wetting states is obtained. It can describe the jumping motion under various wetting conditions, which is validated by some experimental results. This work provides theoretical insights into the accurate control of the electrowetting-induced jumping motion of droplets on textured hydrophobic surfaces.

I. INTRODUCTION

Droplets jumping on hydrophobic surfaces have attracted researchers' attention due to their potential applications in many industrial fields, such as anti-icing,[1] anti-dew,[2] self-cleaning,[3] and heat and mass transfer enhancement.[4–6] Droplets can jump from solid substrates in many cases. In nature, coalescence-induced jumping motion on hydrophobic substrates was discovered and has been investigated in theoretical,[7] experimental,[8] and numerical studies.[9,10] In industrial fields, electrowetting is found to be one of the most efficient techniques for manipulating droplets so that they move on or jump off hydrophobic surfaces.[11,12] This method has been used for accurately controlling droplets in many microfluidic applications.[13,14] In particular, many researchers have concentrated on understanding the dynamic mechanisms in the electrowetting-induced jumping motion of droplets on hydrophobic substrates. Lee *et al.*[15,16] investigated the jumping mechanisms with regard to the jumping height and energy conversion on superhydrophobic surfaces. They suggested that the detachment of these droplets could be improved by tuning the wettability of the substrates or by increasing the frequency of the square pulse

signals. Raman *et al.*[17,18] simulated the electrowetting-induced droplet ejection on solid substrates in which the dependence of their jumping behavior on pulse characteristics is investigated. Based on their simulations in the lattice Boltzmann method, the viscous dissipation that occurs during the detachment can be increased by using a higher voltage. They also investigated droplet ejection dynamics under shear flow and confirmed that the droplet angle of flight, aspect ratio, and surface energy are found to increase with an increase in the applied voltage. Cavalli *et al.*[19] experimentally investigated electrowetting-induced droplet detachment on solid surfaces and analyzed the energy dissipation during retraction. They investigated the efficiency of energy conversion between the surface energy and the gravitational potential energy of the droplet after the jump. Their results indicated that the finite wettability of substrates can affect their detachment dynamics, and they proposed a novel rationale for the previously reported large critical radius for droplet detachment from micro-textured substrates. Wang *et al.*[20] analytically investigated the droplet electrowetting phenomenon on heterogeneous substrates and validated their model by experiments. Xu *et al.*[21] confirmed that a bubble underneath liquid water can also detach by an electrowetting-driven interfacial wave. Vo *et al.*[22,23] experimentally investigated the critical conditions including viscosity of the work liquid and the droplet size under which droplets would jump off the solid substrates. Their analysis demonstrated the effects of contact-line pinning on the dynamic process of the electrowetting-induced jumping of droplets. Zhang *et al.*[24] derived a closed-form formula to describe the energy transition when a droplet jumps off a flat hydrophobic substrate based on the energy conversion of the droplet–substrate system. The model can accurately predict the electrowetting-induced jumping velocity of droplets on flat hydrophobic substrates with a range of wettabilities. Their results were in good agreement with previous experimental and numerical studies. They also confirmed their theory with many-body dissipative particle dynamics, which has been widely used to investigate microfluidic dynamic processes in many applications with free interfaces including liquid cylinder pinchoff[25,26] and droplet wetting dynamics on solid surfaces.[27–31] Zheng *et al.*[32] investigated droplet impacting dynamics on a surface with adjustable wettability based on the dielectrowetting effect. Their experiments identified four different impact phenomena of the drop and provided the corresponding phase diagrams. Also, their results implied that during the dynamic process, the bubble maximum spreading factor and spreading time are controlled by the Weber number. Du *et al.*[33] introduced the gravity potential to correct the prediction of energy conversion, which provides a clearer explanation for droplet electrowetting on flat solid substrates. However, a full understanding of the phenomenon of electrowetting of droplets on textured hydrophobic substrates for different initial wetting and electrowetting states remains unclear. Moreover, the effects of wetting states on the accurate prediction of the droplet escape velocity from solid surfaces need further systematic study. In this work, we present a theoretical expression of the electrowetting-induced jumping velocity of a liquid droplet on textured hydrophobic surfaces with different wetting and electrowetting states, which can provide more insight into the electrowetting of droplets on natural solid surfaces and be more helpful for directing the design of multifunctional microfluidic devices.

II. THEORY AND DISCUSSIONS

Specifically, we consider wetting a liquid droplet on a textured hydrophobic substrate. The natural wetting states could be Cassie–Baxter state and Wenzel state with static contact angles θ_{CB} and θ_W, respectively, as shown in Figs. 1(a) and 1(b), which are related to the texture parameters and chemical contents of the substrates.[34] Figure 1(c) shows a droplet in the Wenzel state that is transferred from the natural Cassie–Baxter state. In this case, the changed contact angle (θ'_W) is usually different from that of the natural Wenzel state. When a voltage is applied between the droplet and the substrate, the Maxwell stress concentrated on the triple-phase contact line can break the intrinsic balance between the three-phase interfacial tensions to deform the droplet. The related experimental studies[22,23] show that the voltage from 60 to 120 V can generate the changed electrowetting contact angles with a range from 60° to 120° and that the spreading radius of droplets, the liquid viscosity, and the electrowetting level can lead to combined effects on the electrowetting contact angle and the energy stored in the droplets at the equilibrium electrowetting state. In this work, the conditions for the electrowetting level are similar to that mentioned above. Also, the work liquid is taken as a pure conductor.[35] When the applied voltage is turned off, the energy stored in the droplet surface during the deformation can make the droplet retract and even jump from the substrates. Here, the effect of gravity is neglected in the derivations as we assume that the droplets are much smaller than the capillary length $l_c = (\gamma/\rho g)^{(1/2)}$, where γ, g, and ρ are the liquid–vapor surface tension, the acceleration due to gravity, and the density of the liquid. For water droplets, $l_c \approx 2.7$ mm.

Corresponding to different wetting states, the apparent contact angles can be described by models derived from Young's equation,[36] i.e., the Cassie–Baxter equation[37] and the Wenzel equation.[38] The surface energy of droplets is related to the three-phase interaction at the interfaces.[34]

In particular, for a droplet in the Cassie–Baxter wetting state with an apparent contact angle θ_{CB}, we assume that the volume of the droplet V_l is constant. The wetting radius is $R_{CB} = [3V_l/(\pi(2 - 3\cos\theta_{CB} + \cos^3\theta_{CB}))]^{1/3}$. Then, the surface energy of the droplet in the Cassie–Baxter state E_{CB} is

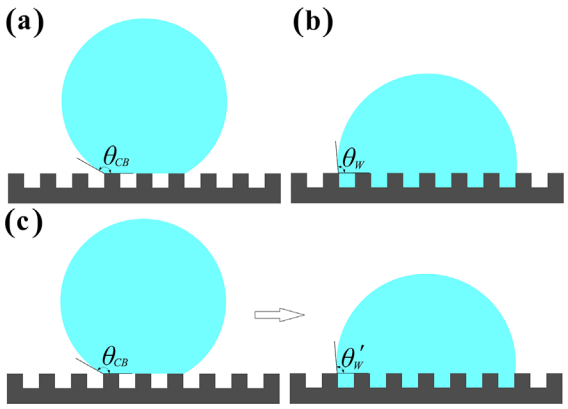

FIG. 1. Schematic of wetting a droplet on textured hydrophobic substrates: (a) the Cassie–Baxter state (θ_{CB}), (b) the Wenzel state (θ_W), and (c) the Wenzel state transitioned from the Cassie–Baxter state (θ'_W).

$$E_{CB} = \gamma A_{lv} + \gamma_{sl} A_{sl} + \gamma_{sv}(\Lambda - A_{sl}) = \gamma \pi R_{CB}^2 \left[2(1 - \cos\theta_{CB}) - \cos\theta_{CB} \sin^2\theta_{CB}\right] + \gamma_{sv}\Lambda, \quad (1)$$

where γ is the liquid–vapor interface tension. γ_{sl} and γ_{sv} represent the solid–liquid and solid–vapor interface tensions, respectively. Λ is the total area of the solid surface including the solid–vapor and solid–liquid interfaces. A_{lv} and A_{sl} are the surface areas of the liquid–vapor and solid–liquid interfaces, respectively.

For a droplet in the Wenzel state with an apparent contact angle θ_W, the wetting radius is $R_W = [3V_l/(\pi(2 - 3\cos\theta_W + \cos^3\theta_W))]^{1/3}$. In this case, the surface energy E_W is

$$E_W = \gamma A_{lv} + \gamma_{sl} A_{sl} + \gamma_{sv}(\Lambda - A_{sl}) = \gamma \pi R_W^2 \left[2(1 - \cos\theta_W) - \cos\theta_W \sin^2\theta_W\right] + \gamma_{sv}\Lambda. \quad (2)$$

The surface energy of droplets in the Cassie–Baxter state is much higher than in the Wenzel state. If there are small external disturbances, a wetting transition could occur from the Cassie–Baxter state to the Wenzel state. In that case, the static contact angle can change, which is marked as θ'. The corresponding surface energy E'_W is then

$$E'_W = \gamma A_{lv} + \gamma_{sl} A_{sl} + \gamma_{sv}(\Lambda - A_{sl}) = \gamma \pi R'^2_W \left[2\left(1 - \cos\theta'_W\right) - \cos\theta'_W \sin^2\theta'_W\right] + \gamma_{sv}\Lambda, \quad (3)$$

where $R'_W = [3V_l/(\pi(2 - 3\cos\theta'_W + \cos^3\theta'_W))]^{1/3}$ is the radius of a droplet with a spherical cap.

In electrowetting, an external voltage U is applied between the droplet and the substrate. This causes the droplet to spread over the surface so that the apparent contact angle experiences a significant reduction. This is because the solid–liquid interface tension is reduced by the Maxwell stress concentrated on the triple-phase contact line.[39,40] Wang and Zhao[41] investigated the relation between the spreading equilibrium state, which has a smaller contact angle θ_E, and the heterogeneity of the textured substrates. Until saturation of the contact angle occurs, it is given by the modified Lippmann–Young equation,

$$\cos\theta_E = f_1\left(\cos\theta_Y + \frac{1}{2}\frac{\varepsilon U^2}{d\gamma_{lv}}\right) - f_2, \quad (4)$$

where ε is the electrical permittivity and d is the thickness of the insulating layer. The heterogeneous coefficients of the substrates are given by $f_1 = \alpha\beta(1 + \lambda)$ and $f_2 = 1 - \alpha\beta$. The substrates in our model are all isotropic, i.e., $\lambda = 1$. α and β are coefficients for the wetting state of droplets on textured substrates. If $\beta = 1$, the droplet is in the Cassie–Baxter state, and the electrowetting contact angle is marked as θ_{E-CB}. The electrowetting radius is $R_{E-CB} = [3V_l/(\pi(2 - 3\cos\theta_{E-CB} + \cos^3\theta_{E-CB}))]^{1/3}$. If $\alpha = 1$, the droplet is in the Wenzel state. The electrowetting contact angle is marked as θ_{E-W}. The electrowetting radius is then $R_{E-W} = [3V_l/(\pi(2 - 3\cos\theta_{E-W} + \cos^3\theta_{E-W}))]^{1/3}$.

If the applied voltage is suddenly turned off, since the relaxation time of the droplet is much larger than the characteristic discharge time for interfacial charges, the shape of the droplet remains the same, with the same apparent electrowetting contact angle θ_E, as there is no Maxwell stress interacting on the triple-phase contact line. However, for droplets initially in the Cassie–Baxter state, when the voltage is turned off, the wetting state could be either the Cassie–Baxter state or the Wenzel state. In contrast, droplets initially in the Wenzel state do not change their wetting state when the voltage is turned off. Thus, there are three cases for the surface energy E_{EW} of a droplet after the voltage is turned off:

1. For a droplet in the Cassie–Baxter state, initially and also during electrowetting, the surface energy E_{CB-CB} is

$$E_{CB-CB} = \gamma A'_{lv} + \gamma_{sl} A'_{sl} + \gamma_{sv}\left(\Lambda - A'_{sl}\right) = \gamma \pi R_{E-CB}^2 \left[2(1 - \cos\theta_{E-CB}) - \cos\theta_{CB} \sin^2\theta_{E-CB}\right] + \gamma_{sv}\Lambda, \quad (5)$$

   where A'_{lv} and A'_{sl} represent the liquid–vapor and solid–liquid areas after the electrowetting, respectively. The electrowetting contact angle is marked as θ_{E-CB}. θ_{CB} is the initial contact angle, which is due to the interaction at the solid–liquid interface after the voltage is turned off.
2. For a droplet initially in the Cassie–Baxter state that was induced into transitioning to the Wenzel state by the electrowetting interaction, the surface energy is

$$E_{CB-W} = \gamma A'_{lv} + \gamma_{sl} A'_{sl} + \gamma_{sv}\left(\Lambda - A'_{sl}\right) = \gamma \pi R'^2_{E-W} \left[2\left(1 - \cos\theta'_{E-W}\right) - \cos\theta'_W \sin^2\theta'_{E-W}\right] + \gamma_{sv}\Lambda, \quad (6)$$

   where θ'_W is the contact angle in the Wenzel state after transitioning from the Cassie–Baxter state. θ'_{E-W} is the electrowetting contact angle. The corresponding electrowetting radius of the droplet is

$$R'_{E-W} = \left[3V_l/\left(\pi\left(2 - 3\cos\theta'_{E-W} + \cos^3\theta'_{E-W}\right)\right)\right]^{1/3}.$$

3. For a droplet in the Wenzel state, the surface energy E_{W-W} is

$$E_{W-W} = \gamma A'_{lv} + \gamma_{sl} A'_{sl} + \gamma_{sv}\left(\Lambda - A'_{sl}\right) = \gamma \pi R_{E-W}^2 \left[2(1 - \cos\theta_{E-W}) - \cos\theta_W \sin^2\theta_{E-W}\right] + \gamma_{sv}\Lambda. \quad (7)$$

When the droplet retracts, the viscous dissipation E_{vis} in the bulk droplet can be approximately estimated as[24,42,43]

$$E_{vis} = 16\pi\mu\sqrt{\frac{\gamma R_0^3}{\rho}}, \quad (8)$$

where R_0 is the initial radius of the droplet. μ and ρ are the viscosity and the density of the liquid, respectively. A detailed derivation and analysis of the parameters can be found in our previous work,[24] in which we confirmed that the viscous dissipation changes with the liquid–vapor interface tension and the initial radius of the droplet but is independent of the jumping velocity and the initial wetting contact angle.

As the contact line on a heterogeneous substrate recedes, the liquid interface experiences a pinning and depinning process and then elastic energy is generated.[44,45] The elastic force per unit length along the contact line is $f \approx \pi \sin^2\theta_r \gamma \ln^{-1} LP^{-1}$, where θ_r is the receding contact angle after the voltage is turned off, which is estimated to be a constant and independent of the electrowetting contact angle.[23] L is estimated to be the droplet radius R_0, which represents the macroscopic cutoff length of the contact line region. P is the defect size,

which is dependent on the roughness and chemical heterogeneity of the substrate. For droplets in different wetting states, the elastic energy related to oscillations of the contact line can be estimated by integrating f over the area swept by the contact line $S_{cl} = \pi R_E^2$ as follows:

$$E_{cl} = fS_{cl} = \frac{\pi \sin^2 \theta_r}{\ln LP^{-1}} \gamma \pi R_E^2, \tag{9}$$

where r_f is the ratio of the real contact area at the solid–liquid interface and its projection.

During retraction, if the residual energy can overcome the dissipation and adhesion interaction, the droplet jumps off the substrate. The surface energy of the droplet is then estimated as

$$E_{free} = \gamma 4\pi R_0^2 + \gamma_{sv}\Lambda. \tag{10}$$

From energy conservation, $E_{EW} = E_{vis} + E_{cl} + E_{free} + E_k$. The kinetic energy of the droplet E_k can be derived for different initial wetting and electrowetting states as follows:

1. For a droplet in the Cassie–Baxter state, initially and also during electrowetting,

$$E_{k-CB-CB} = \gamma \pi R_{E-CB}^2 \left[2(1 - \cos\theta_{E-CB}) - \cos\theta_{CB} \sin^2 \theta_{E-CB}\right] - 16\pi\mu\sqrt{\frac{\gamma R_0^3}{\rho}} - \frac{\pi \sin^2 \theta_r}{\ln LP^{-1}} \gamma \pi R_{E-CB}^2 - \gamma 4\pi R_0^2. \tag{11}$$

2. For a droplet initially in the Cassie–Baxter state that transitions into the Wenzel state due to electrowetting,

$$E_{k-CB-W} = \gamma \pi R'^2_{E-W} \left[2\left(1 - \cos\theta'_{E-W}\right) - \cos\theta'_W \sin^2 \theta'_{E-W}\right] - 16\pi\mu\sqrt{\frac{\gamma R_0^3}{\rho}} - \frac{\pi \sin^2 \theta_r}{\ln LP^{-1}} \gamma \pi R'^2_{E-W} - \gamma 4\pi R_0^2. \tag{12}$$

3. For a droplet in the Wenzel state,

$$E_{k-W-W} = \gamma \pi R_{E-W}^2 \left[2(1 - \cos\theta_{E-W}) - \cos\theta_W \sin^2 \theta_{E-W}\right] - 16\pi\mu\sqrt{\frac{\gamma R_0^3}{\rho}} - \frac{\pi \sin^2 \theta_r}{\ln LP^{-1}} \gamma \pi R_{E-W}^2 - \gamma 4\pi R_0^2. \tag{13}$$

Thus, the jumping velocity V_J of droplets for different electrowetting states can be obtained:

1. For a droplet in the Cassie–Baxter state, initially and also during electrowetting,

$$V_{CB-CB} = u\left[\frac{3}{2}A(\theta_{CB}, \theta_{E-CB}, \theta_r) - 6(1 + 4Oh)\right]^{1/2}, \tag{14}$$

where the Ohnesorge number is defined as $Oh = \mu/(\rho\sigma_{lv}R)^{1/2}$ and the electrowetting coefficient

$$A(\theta_{CB}, \theta_{E-CB}, \theta_r) = \sqrt[3]{\left(\frac{4}{2 - 3\cos\theta_{E-CB} + \cos^3\theta_{E-CB}}\right)^2} \times \left[2(1 - \cos\theta_{E-CB}) - \cos\theta_{CB}\sin^2\theta_{E-CB} - \frac{\pi \sin^2\theta_r}{\ln LP^{-1}}\right].$$

The characteristic capillary velocity $u = \sqrt{\gamma/\rho R_0}$.[46]

2. For a droplet initially in the Cassie–Baxter state that transitions into the Wenzel state due to electrowetting,

$$V_{CB-W} = u\left[\frac{3}{2}A\left(\theta'_W, \theta'_{E-W}, \theta_r\right) - 6(1 + 4Oh)\right]^{1/2}, \tag{15}$$

where

$$A\left(\theta'_W, \theta'_{E-W}, \theta_r\right) = \sqrt[3]{\left(\frac{4}{2 - 3\cos\theta'_{E-W} + \cos^3\theta'_{E-W}}\right)^2} \times \left[2\left(1 - \cos\theta'_{E-W}\right) - \cos\theta'_W \sin^2\theta'_{E-W} - \frac{\pi \sin^2\theta_r}{\ln LP^{-1}}\right].$$

3. For a droplet in the Wenzel state,

$$V_{W-W} = u\left[\frac{3}{2}A(\theta_W, \theta_{E-W}, \theta_r) - 6(1 + 4Oh)\right]^{1/2}, \tag{16}$$

where

$$A(\theta_W, \theta_{E-W}, \theta_r) = \sqrt[3]{\left(\frac{4}{2 - 3\cos\theta_{E-W} + \cos^3\theta_{E-W}}\right)^2} \times \left[2(1 - \cos\theta_{E-W}) - \cos\theta_W \sin^2\theta_{E-W} - \frac{\pi \sin^2\theta_r}{\ln LP^{-1}}\right].$$

We can combine these formulas into the following unified expression:

$$V_J = u\left[\frac{3}{2}A(\theta, \theta_E, \theta_r) - 6(1 + 4Oh)\right]^{1/2}, \tag{17}$$

where

$$A(\theta, \theta_E, \theta_r) = \sqrt[3]{\left(\frac{4}{2 - 3\cos\theta_E + \cos^3\theta_E}\right)^2} \times \left[2(1 - \cos\theta_E) - \cos\theta \sin^2\theta_E - \frac{\pi \sin^2\theta_r}{\ln LP^{-1}}\right],$$

where θ is the natural wetting contact angle; θ_E is the electrowetting contact angle; and θ_r is the specific receding contact angle, which needs to be measured after the droplet has receded when the voltage is turned off. For different wetting conditions, the corresponding electrowetting-induced jumping velocity V_J can be calculated for a droplet on different substrates given the angles as follows:

- Flat hydrophobic substrates: $\theta = \theta_Y$, where θ_Y is the intrinsic contact angle of the substrate, and $\theta_E = \theta_{E-Y}$, where θ_{E-Y} is the electrowetting contact angle of the droplet on the flat substrate. These relations were proposed in our previous work,[24] if the elastic energy of the contact line can be neglected.
- Textured substrates where the droplet is in the natural or the electrowetting Cassie–Baxter state: $\theta = \theta_{CB}$ and $\theta_E = \theta_{E-CB}$.
- Textured substrates where the droplet is in the Cassie–Baxter state initially and then transitions into the Wenzel state due to the electrowetting interaction: $\theta = \theta_{CB}$ and $\theta_E = \theta'_{E-W}$.

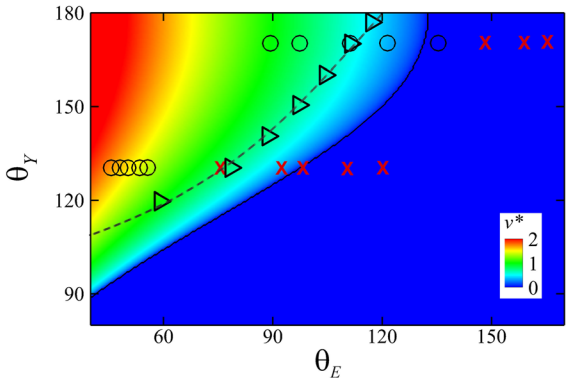

FIG. 2. Comparison with experimental results[19] and the previous theory (the cloud and the solid line).[24] [Reproduced from K. Zhang *et al.*, Phys. Fluids **31**, 081703 (2019) with the permission of AIP Publishing.] Dashed line and triangle signals represent the prediction of droplet detachment from this theory in which the dynamic receding contact angle is calculated as $\theta_r \approx 121^\circ$ and the parameter P of the flat surfaces can be approximated at 6×10^{-10} m.[22,23]

- Textured substrates where the droplet is in the Wenzel state: $\theta = \theta_W$ and $\theta_E = \theta_{E-W}$.

This model can predict the droplet jumping motion for different wetting states with various contact angles θ and electrowetting contact angles θ_E, as shown in Fig. 2. It gives the critical condition for the jumping motion of droplets with a given *Oh* number and the dimensionless jumping velocity of the droplet, which is scaled by the characteristic capillary velocity u, i.e., $v^* = V_J/u$.

III. CONCLUSIONS

In summary, this work is an analytical investigation of the energy conversion between surface energy and kinetic energy due to viscous dissipation during electrowetting-induced jumping motion of droplets on textured hydrophobic substrates in different wetting states. The theory for droplets on flat hydrophobic substrates is extended to describe the electrowetting-induced detachment of droplets on textured hydrophobic substrates, based on the relation between the electrowetting-induced velocity, the Cassie–Baxter or Wenzel contact angle, the modified Lippmann–Young contact angle, and the *Oh* number. The elastic energy of the triple-phase contact line is also taken into consideration. The effects of natural and electrowetting states on the jumping velocity of droplets are discussed and corresponding analytical predictions for the electrowetting-induced velocity are given. A unified form for predicting the electrowetting-induced jumping velocity of droplets on both flat and textured substrates in different wetting states is obtained. This model describes the jumping motion for various wetting conditions. Gravity is neglected, so that this model is applicable for micro- and nano-droplets whose size is much smaller than the capillary length. This work may provide new insights into the accurate control of the electrowetting-induced jumping motion of droplets on textured hydrophobic substrates.

SUPPLEMENTARY MATERIAL

See the supplementary material for an illustration of droplet radius before and after the voltage is applied as well as the energy of droplet surface is provided.

ACKNOWLEDGMENTS

This work was supported by the National Natural Science Foundation of China (Grant Nos. 11872283, 12102218, and 12002212).

AUTHOR DECLARATIONS

Conflict of Interest

The authors have no conflicts to disclose.

DATA AVAILABILITY

Data sharing is not applicable to this article as no new data were created or analyzed in this study.

REFERENCES

[1]J. B. Boreyko and C. P. Collier, "Delayed frost growth on jumping-drop superhydrophobic surfaces," ACS Nano **7**, 1618–1627 (2013).
[2]J. B. Boreyko and C. H. Chen, "Self-propelled dropwise condensate on superhydrophobic surfaces," Phys. Rev. Lett. **103**, 184501 (2009).
[3]K. M. Wisdom, J. A. Watson, X. Qu, F. Liu, G. S. Watson, and C.-H. Chen, "Self-cleaning of superhydrophobic surfaces by self-propelled jumping condensate," Proc. Natl. Acad. Sci. U. S. A. **110**, 7992–7997 (2013).
[4]N. Miljkovic, R. Enright, Y. Nam, K. Lopez, N. Dou, J. Sack, and E. N. Wang, "Jumping-droplet-enhanced condensation on scalable superhydrophobic nanostructured surfaces," Nano Lett. **13**, 179–187 (2013).
[5]K. F. Wiedenheft, H. A. Guo, X. Qu, J. Boreyko, F. Liu, K. Zhang, F. Eid, A. Choudhury, Z. Li, and C.-H. Chen, "Hotspot cooling with jumping-drop vapor chambers," Appl. Phys. Lett. **110**, 141601 (2017).
[6]J. Oh, P. Birbarah, T. Foulkes, S. L. Yin, M. Rentauskas, J. Neely, R. C. N. Pilawa-Podgurski, and N. Miljkovic, "Jumping-droplet electronics hot-spot cooling," Appl. Phys. Lett. **110**, 123107 (2017).
[7]R. Enright, N. Miljkovic, J. Sprittles, K. Nolan, R. Mitchell, and E. N. Wang, "How coalescing droplets jump," ACS Nano **8**, 10352–10362 (2014).
[8]F. Liu, G. Ghigliotti, J. J. Feng, and C.-H. Chen, "Self-propelled jumping upon drop coalescence on Leidenfrost surfaces," J. Fluid Mech. **752**, 22–38 (2014).
[9]F. Liu, G. Ghigliotti, J. J. Feng, and C.-H. Chen, "Numerical simulations of self-propelled jumping upon drop coalescence on non-wetting surfaces," J. Fluid Mech. **752**, 39–65 (2014).
[10]K. Zhang, Z. Li, M. Maxey, S. Chen, and G. E. Karniadakis, "Self-cleaning of hydrophobic rough surfaces by coalescence-induced wetting transition," Langmuir **35**, 2431–2442 (2019).
[11]V. Bahadur and S. V. Garimella, "An energy-based model for electrowetting-induced droplet actuation," J. Micromech. Microeng. **16**, 1494 (2006).
[12]Z. Li, Z. W. Zhou, and G. Hu, "Dissipative particle dynamics simulation of droplet oscillations in ac electrowetting," J. Adhes. Sci. Technol. **26**, 1883–1895 (2012).
[13]Y. P. Zhao and Y. Wang, "Fundamentals and applications of electrowetting: A critical review," Rev. Adhes. Adhes. **1**, 114–174 (2013).
[14]S. Arscott, "Electrowetting and semiconductors," RSC Adv. **4**, 29223–29238 (2014).
[15]S. J. Lee, J. Hong, K. H. Kang, I. S. Kang, and S. J. Lee, "Electrowetting-induced droplet detachment from hydrophobic surfaces," Langmuir **30**, 1805–1811 (2014).
[16]S. J. Lee, S. Lee, and K. H. Kang, "Droplet jumping by electrowetting and its application to the three-dimensional digital microfluidics," Appl. Phys. Lett. **100**, 081604 (2012).
[17]K. A. Raman, R. K. Jaiman, T. S. Lee, and H. T. Low, "A numerical study on electrowetting-induced jumping and transport of droplet," Int. J. Heat Mass Transfer **99**, 805–821 (2016).
[18]K. A. Raman, E. Birgersson, Y. Sui, and A. Fisher, "Electrically induced droplet ejection dynamics under shear flow," Phys. Fluids **32**, 032103 (2020).
[19]A. Cavalli, D. J. Preston, E. Tio, D. W. Martin, N. Miljkovic, E. N. Wang, F. Blanchette, and J. W. M. Bush, "Electrically induced drop detachment and ejection," Phys. Fluids **28**, 022101 (2016).

[20]Z. Wang, D. van den Ende, A. Pit, R. Lagraauw, D. Wijnperlé, and F. Mugele, "Jumping drops on hydrophobic surfaces, controlling energy transfer by timed electric actuation," Soft Matter **13**, 4856–4863 (2017).
[21]H. Xu, R. Yan, S. Wang, and C.-L. Chen, "Bubble detachment assisted by electrowetting-driven interfacial wave," Phys. Fluids **29**, 102105 (2017).
[22]Q. Vo, H. Su, and T. Tran, "Universal transient dynamics of electrowetting droplets," Sci. Rep. **8**, 836 (2018).
[23]Q. Vo and T. Tran, "Critical conditions for jumping droplet," Phys. Rev. Lett. **123**, 024502 (2019).
[24]K. Zhang, Z. Li, and S. Chen, "Analytical prediction of electrowetting-induced jumping motion for droplets on hydrophobic substrates," Phys. Fluids **31**, 081703 (2019).
[25]M. Arienti, W. Pan, X. Li, and G. Karniadakis, "Many-body dissipative particle dynamics simulation of liquid/vapor and liquid/solid interactions," J. Chem. Phys. **134**, 204114 (2011).
[26]J. Zhao, S. Chen, K. Zhang, and Y. Liu, "A review of many-body dissipative particle dynamics (MDPD): Theoretical models and its applications," Phys. Fluids **33**, 112002 (2021).
[27]Z. Li, G.-H. Hu, Z.-L. Wang, Y.-B. Ma, and Z.-W. Zhou, "Three dimensional flow structures in a moving droplet on substrate: A dissipative particle dynamics study," Phys. Fluids **25**, 072103 (2013).
[28]Y. X. Wang and S. Chen, "Numerical study on droplet sliding across micropillars," Langmuir **31**, 4673–4677 (2015).
[29]J. Y. Zhao and S. Chen, "Following or against topographic wettability gradient: Movements of droplets on a micropatterned surface," Langmuir **33**, 5328–5335 (2017).
[30]D. Y. Pan, G. Zhao, Y. Lin, and X. Shao, "Mesoscopic modelling of microbubble in liquid with finite density ratio of gas to liquid," Europhys. Lett. **122**, 20003 (2018).
[31]C. Lin, D. Cao, D. Zhao, P. Wei, S. Chen, and Y. Liu, "Dynamics of droplet impact on a ring surface," Phys. Fluids **34**, 012004 (2022).
[32]J. Zheng, Y. Cheng, Y. Huang, S. Wang, L. Liu, and G. Chen, "Drop impacting on a surface with adjustable wettability based on the dielectrowetting effect," Phys. Fluids **32**, 097108 (2020).
[33]J. Du, N. T. Chamakos, A. G. Papathanasiou, Y. Li, and Q. Min, "Jumping velocity of an electrowetting-actuated droplet: A theoretical and numerical study," Phys. Rev. Fluids **6**, 123603 (2021).
[34]A. Marmur, "Wetting on hydrophobic rough surfaces: To be heterogeneous or not to be?," Langmuir **19**, 8343–8348 (2003).
[35]W. Welters and L. Fokkink, "Fast electrically switchable capillary effects," Langmuir **14**, 1535–1538 (1998).
[36]T. Young, "An essay on the cohesion of fluids," Philos. Trans. R. Soc. B **95**, 65–87 (1805).
[37]A. B. D. Cassie and S. Baxter, "Wettability of porous surfaces," Trans. Faraday Soc. **40**, 546–551 (1944).
[38]R. N. Wenzel, "Resistance of solid surfaces to wetting by water," Ind. Eng. Chem. **28**, 988–994 (1936).
[39]A. Quinn, R. Sedev, and J. Ralston, "Contact angle saturation in electrowetting," J. Phys. Chem. B **109**, 6268–6275 (2005).
[40]J. M. Oh, S. H. Ko, and K. H. Kang, "Analysis of electrowetting-driven spreading of a drop in air," Phys. Fluids **22**, 032002 (2010).
[41]Z. Wang and Y.-P. Zhao, "Wetting and electrowetting on corrugated substrates," Phys. Fluids **29**, 067101 (2017).
[42]F.-C. Wang, F. Yang, and Y. P. Zhao, "Size effect on the coalescence-induced self-propelled droplet," Appl. Phys. Lett. **98**, 053112 (2011).
[43]C. Lv, P. Hao, Z. Yao, Y. Song, X. Zhang, and F. He, "Condensation and jumping relay of droplets on lotus leaf," Appl. Phys. Lett. **103**, 021601 (2013).
[44]P. G. de Gennes, "Wetting: Statics and dynamics," Rev. Mod. Phys. **57**, 827–863 (1985).
[45]M. Delmas, M. Monthioux, and T. Ondar ç uhu, "Contact angle hysteresis at the nanometer scale," Phys. Rev. Lett. **106**, 136102 (2011).
[46]Y. P. Zhao and Q. Z. Yuan, "Statics and dynamics of electrowetting on pillar-arrayed surfaces at the nanoscale," Nanoscale **7**, 2561–2567 (2015).